Journal of Cell Science 111, 149-159 (1998)
Printed in Great Britain © The Company of Biologists Limited 1998
JCS4456

Genes that cause aberrant cell morphology by overexpression in fission yeast: a role of a small GTP-binding protein Rho2 in cell morphogenesis

Dai Hirata[1,*], Kentaro Nakano[2], Mikiko Fukui[1], Hiroshi Takenaka[1], Tokichi Miyakawa[1] and Issei Mabuchi[2,3]

[1]Department of Molecular Biotechnology, Graduate School of Engineering, Hiroshima University, Higashi-Hiroshima 739, Japan
[2]Graduate Program in Biophysics and Biochemistry, School of Science, University of Tokyo, Hongo, Bunkyo-ku, Tokyo 113, Japan
[3]Department of Life Sciences, Graduate School of Arts and Sciences, University of Tokyo, Meguro-ku, Tokyo 113, Japan
*Author for correspondence (e-mail: dhirata@ipc.hiroshima-u.ac.jp)

Accepted 27 October 1997: published on WWW 23 December 1997

SUMMARY

To identify the genes involved in cell morphogenesis in *Schizosaccharomyces pombe*, we screened for the genes that cause aberrant cell morphology by overexpression. The isolated genes were classified on the basis of morphology conferred. One of the genes causing a rounded morphology was identified as the *rho2*$^+$ gene encoding a small GTP-binding protein. The overexpression of *rho2*$^+$ resulted in a randomized distribution of cortical F-actin and formation of a thick cell wall. Analyses using *cdc* mutants suggested that the overexpression of *rho2*$^+$ prevents the establishment of growth polarity in G_1. The *rho2*$^+$ gene was not essential, but among cells deleted for *rho2*$^+$, those with an irregular shape were observed. The disruptant also showed a defect in cell wall integrity. An HA-Rho2 expressed in the cell was suggested to be present as a membrane-bound form by a cell fractionation experiment. A GFP-Rho2 was localized at the growing end(s) of the cell and the septation site. The localization of GFP-Rho2 during interphase was partially dependent on *sts5*$^+$. These results indicate that Rho2 is involved in cell morphogenesis, control of cell wall integrity, control of growth polarity, and maintenance of growth direction. Analysis of functional overlapping between Rho2 and Rho1 revealed that their functions are distinct from each other, with partial overlapping.

Key words: Cell morphogenesis, F-actin patch, Fission yeast, Rho

INTRODUCTION

Cell morphogenesis is a fundamental phenomenon that is closely regulated during each developmental stage and cell cycle progression. To understand cell morphogenesis, we have initiated a genetic analysis in the unicellular organism, the genetically amenable fission yeast, *Schizosaccharomyces pombe*. The *S. pombe* cell has a cylindrical rod shape of 8-14 μm in length and 3 μm in diameter (Mitchison, 1970). Cell growth occurs only at the ends and the growth polarity dynamically changes in three stages during the cell cycle progression. The first stage is the initiation of growth when cortical F-actin moves from the new end of the cell, which is newly produced by cytokinesis, to the old end, which already exists in the previous cycle. Following this actin movement, cell growth is initiated only from the old end. The second stage is NETO (new end take off; Mitchison and Nurse, 1985). For NETO to take place, two requirements, completion of S phase and attainment of critical cell size, have to be fulfilled. At 0.34 of the cell cycle, a drastic alteration in growth polarity occurs. F-actin localization dynamically alters from the old end to both ends, and growth at the new end is initiated. After this point, the cell exhibits bi-directional growth. The third stage includes septum formation. At mitosis, cell growth ceases and cortical F-actin patches at both ends disappear. Actin reassembles into an F-actin ring in the middle of the cell body where septation will occur (Marks and Hyams, 1985; Marks et al., 1986). These features make *S. pombe* a good system to study cell morphogenesis.

To understand cell morphogenesis in *S. pombe*, morphological mutants have been isolated (reviewed by Snell and Nurse, 1993; Nurse, 1994; Snell and Nurse, 1994; Matsusaka et al., 1995; Verde et al., 1995; Toda et al., 1996; Yaffe et al., 1996). They are morphologically classified into several groups: spherical, bent, branched, and monopolar growth. From analyses of these mutants, a number of evolutionarily conserved proteins have been identified, including small GTP-binding proteins, protein kinases, protein phosphatases, cytoskeleton-related proteins, and functionally unknown proteins.

The Rho family of GTP-binding proteins, which consists of the Rho, Rac and Cdc42 subfamilies, has been implicated in the regulation of a wide range of biological processes, including cell motility, cell adhesion, cytokinesis, cell morphology, and cell growth (Hall, 1994; Takai et al., 1995). The budding yeast *Saccharomyces cerevisiae* has five Rho-related genes: *RHO1* (Madaule et al., 1987), *RHO2* (Madaule et al., 1987), *RHO3* (Matsui and Toh-e, 1992), *RHO4* (Matsui and Toh-e, 1992) and *CDC42* (Adams et al., 1990; Johnson and Pringle, 1990). The essential gene *RHO1* is a homolog of the mammalian *RhoA* gene. Rho1 is localized at the growth sites, including the bud tip and the cytokinesis site, and is required for the budding

process (Yamochi et al., 1994). Three downstream targets of *RHO1* have been identified: a protein kinase C (*PKC1*) (Nonaka et al., 1995; Kamada et al., 1996), 1,3-β-glucan synthase (Drgonová et al., 1996; Qadota et al., 1996), and *BNI1*, known to be involved in cytokinesis or establishment of cell polarity (Kohno et al., 1996). In *S. pombe*, three Rho-related genes, *cdc42*$^+$ (Fawell et al., 1992; Miller and Johnson, 1994), *rho1*$^+$ (Nakano and Mabuchi, 1995), and *rho2*$^+$ (Nakano and Mabuchi, 1995), have been isolated. It has been shown that Rho1 activates 1,3-β-glucan synthase and is involved in cell morphogenesis (Arellano et al., 1996). However, the role of Rho2 in cell morphogenesis remains to be clarified.

Cell morphogenesis is controlled by information on positioning, movement, and timing. The information on positioning and movement are important for the restriction of the growth site to specific regions and the transfer of the growth polarity, respectively. The information on timing is required to coordinate the expression of the information on positioning and movement with cell cycle progression. The establishment of cell morphogenesis is thought to be produced by orderly functional expression of various molecules. Therefore, cell morphogenesis needs a precise functional balance of these molecules. If this balance is disrupted, cells will have difficulty in forming a normal cell morphology. To identify the molecules involved in cell morphogenesis, on the basis of this assumption, we screened genes that cause aberrant cell morphology by overexpression, from an *S. pombe* cDNA library under the control of the thiamine-repressible *nmt1* promoter. One of the *gam* genes (for gene that causes aberrant cell morphology by overexpression) that causes a rounded morphology was identified as the *rho2*$^+$ gene. In the present study, we show that Rho2 is involved in cell morphogenesis, the maintenance of growth direction, control of growth polarity, and control of cell wall integrity.

MATERIALS AND METHODS

Strains, media and yeast transformation

The *Schizosaccharomyces pombe* strains used in this study are listed in Table 1. Complete medium YPD (1% yeast extract, 2% polypeptone, 2% dextrose), modified synthetic EMM (Moreno et al., 1991), and MEA for conjugation and sporulation (Moreno et al., 1991) were used. The plates contained 2% agar. Standard procedures for *S. pombe* genetics were followed (Moreno et al., 1991). Cell concentration and mass were measured with a Sysmex F-820 (TOA Medical Electronics).

Molecular biological techniques

Standard molecular biological techniques were used for construction of plasmids, DNA sequencing and PCR (Sambrook et al., 1989). DNA sequences were determined using an ALFred DNA sequencer (Pharmacia Biotech Inc.) and PCR was performed using a Zymoreactor II AB-1820 (ATTO). Plasmids used in this study are listed in Table 2.

Disruption of the *rho2*$^+$ gene

The genomic DNA fragment containing the *rho2*$^+$ gene was isolated from an *S. pombe* genomic DNA library using the 0.3 kb *Spe*I-*Afl*II fragment of *rho2*$^+$ cDNA as a probe. The 0.9 kb *Spe*I-*Afl*II fragment containing the *rho2*$^+$ coding region of the genomic *rho2*$^+$ gene was deleted from plasmid pUCgrho2E and replaced with the 1.8 kb *ura4*$^+$ fragment (Grimm et al., 1988), yielding plasmid pgrho2::ura4. A 2.9 kb *Pst*I-*Nde*I fragment containing this deleted version of *rho2*$^+$ was used to transform a diploid KND-1 (Table 1). Stable Ura$^+$ transformants were obtained and Southern hybridization confirmed that the *rho2*$^+$ gene had been deleted as expected. The genomic *rho2*$^+$ sequence is available from the GenBank DNA data base (accession number D83721).

Table 1. Fission yeast strains used in this study

Strain	Genotype
HM123	*h*$^-$ *leu1* (from P. Nurse)
TP108-3D	*h*$^+$ *leu1 ura4 his2* (Toda et al., 1991)
JY741	*h*$^-$ *leu1 ura4 ade6-M216* (from M. Yamamoto)
JY742	*h*$^+$ *leu1 ura4 ade6-M210* (from M. Yamamoto)
KND-1	*h*$^-$/*h*$^+$ *leu1/leu1 ura4/ura4 ade6-M216/ade6-M210*
KN-1	*h*$^-$ *leu1 ura4 ade6 rho2::ura4*$^+$
TP40-5B	*h*$^-$ *leu1 sts5-7* (Toda et al., 1991)
TP47-2B	*h*$^-$ *leu1 pck2/sts6-8* (Toda et al., 1993)
cdc7	*h*$^+$ *cdc7-24* (from P. Nurse)
cdc10	*h*$^+$ *cdc10-129* (from P. Nurse)
cdc25	*h*$^+$ *cdc25-22* (from P. Nurse)
tea1	*h*$^+$ *leu1 ade6-M210 tea1* (from P. Nurse)
DH69-1	*h*$^-$ *leu1 cdc7-24*
DH70-2	*h*$^-$ *leu1 cdc10-129*
DH71-1	*h*$^-$ *leu1 cdc25-22*
DH68-4	*h*$^-$ *leu1 ura4 ade6 cdc10-129 rho2::ura4*$^+$
DH66-1	*h*$^-$ *leu1 ura4 ade6 cdc7-24 rho2::ura4*$^+$
DH67-1	*h*$^-$ *leu1 ura4 cdc25-22 rho2::ura4*$^+$

Assay for the sensitivity of yeast cells to glucanase treatment

The procedures described by Shiozaki and Russell (1995) were followed. β-Glucanase (100 μg/ml, Zymolyase-100T, Seikagaku Co.) was used for digesting the cell wall.

Assay for the sensitivity of yeast cells to aculeacin A and staurosporine

The sensitivity of yeast cells to aculeacine A (Wako Pure Chemical Industries Ltd) and staurosporine (provided by Dr H. Nakano, Kyowa Hakko Co.) was examined by streaking cells on YPD plates containing various concentrations of the drug. After the plates were incubated at 28°C for 3 to 4 days, the drug sensitivity was evaluated by the growth of the cells streaked.

Western blot analysis of Rho2

HA-Rho2 proteins expressed in yeast cells were detected by western blot analysis with 12CA5 mAb (Wilson et al., 1984). Total cell extract was prepared by the method of Matsusaka et al. (1995). Protein samples were run on an SDS-PAGE (Laemmli, 1970) and electrically transferred onto nitrocellulose filters. For detection of HA-Rho2, 12CA5 mAb as a primary antibody and horseradish peroxidase-conjugated sheep anti-mouse IgG (Amersham) as a second antibody were used. The ECL chemiluminescence system (Amersham) was used to detect bound antibody.

Cytological techniques

Cytological techniques were performed according to the method of Alfa et al. (1993) and Matsusaka et al. (1995). For F-actin staining, rhodamine-phalloidin (Molecular Probes Inc.) was used. Calcofluor white (Sigma) was used to monitor cell wall growth, and DAPI (4′,6-diamidino-2-phenylindole) (Sigma) was used for observing chromatin regions.

RESULTS

Screen for genes that cause aberrant cell morphology by overexpression

To isolate a gene involved in cell morphogenesis, *S. pombe*

Table 2. Plasmids used in this study

Plasmid	Characteristics
pREP1	A thiamine-repressible *nmt1* promoter (full strength; induction ratio, 300×), *S. cerevisiae LEU2*, *ars1* (Maundrell, 1990; Basi et al., 1993; Forsburg et al., 1993)
pREP41	A thiamine-repressible *nmt41* promoter (induction ratio,25×), *LEU2*, *ars1*
pREP81	A thiamine-repressible *nmt81* promoter (induction ratio, 7×), *LEU2*, *ars1*
pFM2345	*nmt1-rho2*$^+$, *LEU2*, *ars1*; isolated by this study from an *S. pombe* cDNA library
pUCgrho2E	Genomic *rho2*$^+$ (isolated from an *S. pombe* genomic library using *rho2*$^+$ cDNA as a probe); made by inserting the 4 kb *Eco*RI-*Eco*RI fragment containing genomic *rho2*$^+$ into the *Eco*RI site of pUC18.
pREP1-Rho2	*nmt1-rho2*$^+$, *LEU2*, *ars1*; made by inserting the 0.6 kb *Sal*I-*Bam*HI PCR fragment containing the entire ORF of *rho2*$^+$ into the *Sal*I-*Bam*HI site of pREP1. The 0.6 kb *rho2*$^+$ DNA fragment was amplified by PCR using two primers RH2NS, 5′-AAAAGTCGACGATGTTGCAATCTCA-3′ and RN2CB, 5′-AAAAGGATCCTTATGAAATGATGCA-3′, where *Sal*I and *Bam*HI sites are underlined.
pREP41-Rho2	*nmt41-rho2*$^+$, *LEU2*, *ars1*; made by inserting the 0.6 kb *Nde*I-*Sac*I fragment containing the entire ORF of *rho2*$^+$ of pET28rho2 into the *Nde*I-*Sac*I site of pREP41.
pREP81-Rho2	*nmt81-rho2*$^+$, *LEU2*, *ars1*; made by inserting the 0.6 kb *Nde*I-*Sac*I fragment containing the entire ORF of *rho2*$^+$ of pET28rho2 into the *Nde*I-*Sac*I site of pREP81.
pREP81-Rho2(G17V)	*nmt81-rho2*(G17V), *LEU2*, *ars1*; made by inserting the 0.5 kb *Spe*I-*Sac*I fragment of pUCrho2G17V into the *Spe*I-*Sac*I site of pREP81-Rho2. pUCrho2G17V was made by inserting the 0.6 kb rho2G17V DNA fragment blunted with Klenow fragment into the *Sma*I site of pUC18. Mutagenesis of *rho2*$^+$ was according to the method of Ito et al. (1991), using R2G17V oligonucleotide, 5′-GTAGGCGATGTTGCCTGCGGG-3′.
pREP1-Rho2(C197S)	*nmt81-rho2*(C197S), *LEU2*, *ars1*; made by inserting the 0.5 kb *Spe*I-*Sac*I fragment of pUCrho2C197S into the *Spe*I-*Sac*I site of pREP81-Rho2. pUCrho2C197S was made by inserting the 0.6 kb rho2C197S DNA fragment blunted with Klenow fragment into the *Sma*I site of pUC18. The 0.6 kb rho2C197S DNA fragment was amplified by PCR using two primers RER2, 5′-GTCATATGTTGCAATCTCAACCGA-3′ and RERB2, 5′-CCGGATCCATTATGAAATGATGCTGCAT-3′, where *Nde*I and *Bam*HI sites are underlined.
pREP1-HA-Rho2	*nmt1-HA-rho2*$^+$, *LEU2*, *ars1*; made by inserting the 99 bp *Sal*I-*Xho*I PCR fragment encoding three copies of an epitope sequence consisting of nine amino acid residues derived from the hemagglutinin of the influenza virus (HA1; Wilson et al., 1984) into the *Sal*I site of pREP1-Rho2. The 99 bp HA DNA fragment was amplified by PCR using two primers HNS2, 5′-GGGGTCGACTATGTACCCATACGAT-3′ and HCX2, 5′-CAGCTCGAGCTAGCGTAATCCGGTA-3′, where the *Sal*I and *Xho*I sites are underlined.
pREP1-GFP-Rho2	*nmt1-GFP-rho2*$^+$, *LEU2*, *ars1*; made by inserting the 720 bp *Sal*I-*Xho*I PCR fragment encoding green fluorescent protein (GFP) from the jellyfish *Aequorea victoria* (Prasher et al., 1992) into the *Sal*I site of pREP1-Rho2. The 720 bp GFP DNA fragment was amplified by PCR using two primers GFNS, 5′-AAAAGTCGACGATGAGTAAAGGAGA-3′ and GFCX, 5′-AAAACTCGAGCTTTTGTATAGTTCA-3′, where the *Sal*I and *Xho*I sites are underlined.
pREP81-GFP-Rho2	*nmt81-GFP-rho2*$^+$, *LEU2*, *ars1*; made by inserting the 1.3 kb *Sal*I-*Bam*HI fragment containing the *GFP-rho2*$^+$ gene of pREP1-GFP-Rho2 into the *Sal*I-*Bam*HI site of pREP81.
pREP1-Rho1	*nmt1-rho1*$^+$, *LEU2*, *ars1*; made by inserting the 0.6 kb *Nde*I-*Bam*HI PCR fragment containing the entire ORF of *rho1*$^+$ into the *Nde*I-*Bam*HI site of pREP1. The 0.6 kb *rho1*$^+$ DNA fragment was amplified by PCR using two primers RH1NN, 5′-GTCATATGGCGACAGAACTTCGC-3′ and RN1CB, 5′-GTGGATCCTTACAACAAGATACAACGC-3′, where *Nde*I and *Bam*HI sites are underlined.
pREP41-Rho1	*nmt41-rho1*$^+$, *LEU2*, *ars1*; made by inserting the 0.6 kb *Nde*I-*Bam*HI fragment containing the entire ORF of *rho1*$^+$ of pREP1-Rho1 into the *Nde*I-*Bam*HI site of pREP41
pREP81-Rho1	*nmt81-rho1*$^+$, *LEU2*, *ars1*; made by inserting the 0.6 kb *Nde*I-*Bam*HI fragment containing the entire ORF of *rho1*$^+$ of pREP1-Rho1 into the *Nde*I-*Bam*HI site of pREP81

wild-type cells were transformed with an *S. pombe* cDNA library (a gift from Dr P. Nurse) under the control of the thiamine-repressible *nmt1* promoter on an EMM plate containing 4 μM thiamine (promoter off). After incubation at 28°C for 3-4 days, the resulting Leu$^+$ transformants were replicated on an EMM plate containing 4 μM thiamine or an EMM plate (promoter on). After incubation at 32°C for 16 hours, morphologically aberrant cells on the EMM plate were visually selected under fluorescence microscopy by staining with calcofluor. Of 13,000 transformants screened, about 1% of transformants showed aberrant cell morphology under the derepressed condition. From the transformants showing the library plasmid-dependent aberrant cell morphology, fifty four plasmids were recovered through *Escherichia coli* transformation and the isolated plasmids were subjected to DNA sequence analysis. Forty three different genes were isolated and designated *gam* (Table 3). The isolated *gam* genes were morphologically classified into several groups (Fig. 1): round or lemon-like (B and C), bent, curved or branched (D and E), abnormal calcofluor staining (F), elongated (G), abnormally septated (H), and huge (I). The frequencies of the branched (E) and other aberrant cells were 5% and more than 20%, respectively. One (original plasmid designated pFM2345) of the *gam* genes causing round morphology was identified as the *rho2*$^+$ gene that encodes a small GTP-binding protein (Nakano and Mabuchi, 1995), and was characterized further in this study. The characterization of other *gam* genes will be reported elsewhere.

Overexpression of the *rho2*$^+$ gene

Wild-type cells bearing pREP1-Rho2 grown in EMM containing 4 μM thiamine showed a normal rod morphology

Table 3. Classification of the *gam* genes based on the effect of the overexpression on cell morphogenesis

Cell morphology	Number of plasmids	Number of genes
Round, spherical	19	15
Lemon-like	6	4
Curved, bent	5	5
Abnormal calcofluor-staining	7	5
Branched	6	5
Elongated	2	2
Huge	1	1
Abnormally septated	5	5
Unclassified	3	1
Total	54	43

(Fig. 2A, a), while the cells grown in EMM showed nonseptated round (Fig. 2A, b) or septated round morphologies (Fig. 2A, c and d). The nuclear chromatin regions of the *rho2*$^+$-overexpressing cells (Fig. 2A, b-d left) were visualized by staining with DAPI. Each cell had basically one nucleus.

DAPI stains the nuclear chromatin region strongly and the cytoplasmic regions weakly. The thickness of the cell wall could be evaluated by comparing the image of the cytoplasmic region (Fig. 2A, left) with that of the whole cell (Fig. 2A, right). The septum of wild-type cells bearing pREP1-Rho2 grown under the derepressed conditions was thicker than that under the repressed conditions (compare a and c in Fig. 2A), indicating that the overexpression of *rho2*$^+$ causes a thick cell wall. To investigate the effect of the overexpression of *rho2*$^+$ in detail, wild-type cells bearing pREP1-Rho2 in EMM containing 4 μM thiamine were transferred into EMM, and changes in cell number, viability, and percentage of cells with round morphology were examined during the culture. After incubation for 12 hours, the growth of the cells became slow and the viability of the cells went down to 25%. Almost no division was observed after 14 hours. The round cells began to accumulate after 12 hours of incubation. After incubation for 16 hours, the population of normal rod cells decreased to 22%. In contrast, aberrant round cells increased to 78% (25% nonseptated and 53% septated). The percentage of septated cells including normal and aberrant cells reached 58% (Table 4), while that of septated cells grown under the repressed condition remained 15% (data not shown). These results indicated that the overexpression of *rho2*$^+$ causes decrease in viability, loss of growth polarity, and increase in the number of septated cells.

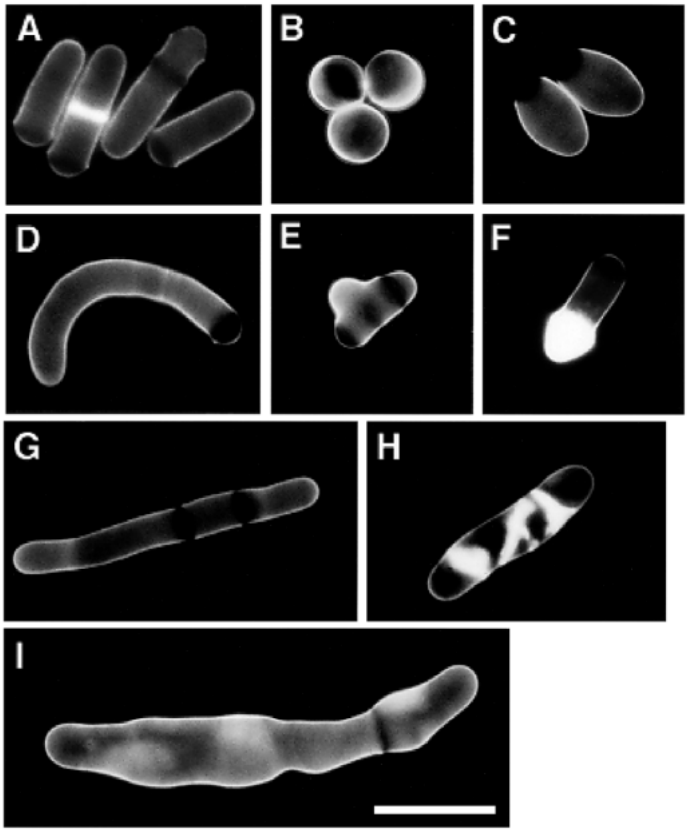

Fig. 1. Morphological categories of the selected transformants. Wild-type (HM123) cells bearing pREP1 (A) or the isolated plasmids, pFM421 (B), pFM2495 (C), pFM168 (D), pFM1548 (E), pFM2926 (F), pFM12973 (G), pFM2845 (H), and pFM3760 (I) were grown in EMM containing 4 μM thiamine at 25°C, transferred into EMM, cultured at 32°C for 16 hours, and stained with calcofluor. Bar, 10 μm.

To examine localization of cortical F-actin in the *rho2*$^+$-overexpressing cells, rhodamine-phalloidin staining was performed. In wild-type cells, cortical F-actin was localized as patches in growing end(s) and the septation site as reported previously (Fig. 2B, a; Marks and Hyams, 1985; Marks et al., 1986). In contrast, in the *rho2*$^+$-overexpressing cells, cortical F-actin was dispersed throughout the cell (Fig. 2B, b), indicating that the overexpression of *rho2*$^+$ causes randomized actin localization. In the septated cells as well, the delocalization of cortical F-actin occurred (Fig. 2B, b, lower cells), suggesting that the growth polarity of the *rho2*$^+$-overexpressing cells is lost during interphase.

Expression of mutated *rho2*$^+$ genes

To examine the effects of expression of mutated *rho2*$^+$ genes on cell morphogenesis, a site-specific mutation was introduced into its GTP-binding or the C-terminal isoprenylation site on the basis of the similarity between Rho2 and mammalian H-Ras. *rho2*(G17V), a constitutively active mutation, was expressed in wild-type cells under the thiamine-repressible *nmt81* promoter whose expression level is much weaker than the *nmt1* promoter (see Table 2). The cells bearing pREP81-Rho2(G17V) grew slowly and showed round morphology (Table 4) with the dispersed cortical F-actin (data not shown), while the cells bearing pREP81-Rho2 grew normally and showed normal rod morphology under the derepressed condition (Table 4). This indicates that the round morphology by the overexpression of *rho2*$^+$ results from increased Rho2 activity. The overexpression of *rho2*(C197S) from the *nmt1* promoter, which would not be isoprenylated by geranylgeranyl transferase, did not affect both cell growth and morphology (Table 4), indicating that the C-terminal isoprenylation of Rho2 is necessary for the function.

Disruption of the *rho2*$^+$ gene

To examine the phenotypic consequence of disruption of the *rho2*$^+$ gene, the one-step gene disruption method (Rothstein, 1983) was carried out (see Materials and Methods for details). The *rho2* disruptant cells grew normally at 20-36°C, indicating that *rho2*$^+$ is not essential for vegetative growth. The disruptant

Table 4. Effect of the expression of the site-specifically mutated *rho2*$^+$ genes on growth and morphology of wild-type cells

			Cell morphology (%)			
			Rod		Round	
Plasmid	Promoter	Growth	Nonseptated	Septated	Nonseptated	Septated
pREP1	*nmt1*	Normal	80	20	0	0
pREP1-Rho2	*nmt1*	Lethal	17	5	25	53
pREP41-Rho2	*nmt41*	Slow	12	5	47	36
pREP81-Rho2	*nmt81*	Normal	77	23	0	0
pREP81-Rho2(G17V)	*nmt81*	Slow	36	9	35	20
pREP1-Rho2(C197S)	*nmt1*	Normal	78	22	0	0

Wild-type (HM123) cells bearing the indicated plasmids grown in EMM containing 4 μM thiamine at 25°C were transferred into EMM and cultured at 30°C for 16 hours.

cells growing at 25°C showed almost normal rod morphology, but 20% of the cells growing at 36°C showed irregular morphology including bent (Fig. 3). In some disruptant cells, calcofluor staining was more intense than in wild-type cells and division scars were not obvious, which were normally stained in the wild-type cells (Fig. 3). In the *rho2* disruptant cells, organization of microtubules seemed to be normal (data not shown).

The overexpression of *rho2*$^+$ caused formation of a thick cell wall as mentioned above. To examine the possibility that Rho2 plays a role in the control of cell wall integrity, we examined the kinetics of cell lysis upon β-glucanase treatment. The *pck2/sts6* mutants defective in cell wall integrity (Toda et al., 1993; Shiozaki and Russell, 1995) were used as control. The *rho2* disruptant cells showed a β-glucanase sensitivity that was intermediate between that of the wild-type and the *pck2* mutant (Fig. 4A). The *rho2*$^+$-overexpressing cells were also more sensitive to the treatment than the wild-type cells (data not shown). The round mutant defective in the *sts5*$^+$ gene (Toda et al., 1996) was also used as control. As described previously (Toda et al., 1996), no difference in the β-glucanase sensitivities of the wild-type and the *sts5* mutant was evident. In the next experiment, we examined the sensitivity of the *rho2* disruptant cells to antibiotics aculeacin A (a specific inhibitor of glucan synthesis) (Miyata et al., 1980), staurosporine (potent inhibitor of protein kinase C) (Nakano et al., 1987), and cycloheximide (inhibitor of protein synthesis). The *pck2* mutant cells showed supersensitivity to all of the drugs examined, and the *sts5* mutant cells showed supersensitivity specific to staurosporine (Fig. 4B). The *rho2* disruptant cells showed supersensitivity to both aculeacin A and staurosporine, but there was no difference in the sensitivity to cycloheximide between wild-type and the *rho2* disruptant cells (Fig. 4B). From these results, it was indicated that the *rho2* disruptant cells have a defect in the control of cell wall integrity.

Double mutant analysis between *rho2* and *cdc* mutants

To determine precisely the cell cycle point when the mutant cells lose normal cell morphology, we constructed *cdcrho2* double mutants between the *rho2* disruptant and temperature-sensitive *cdc* mutants: *cdc10-129*, which arrests in G_1; *cdc25-22*, which arrests in G_2; and *cdc7-24*, a septation mutant which undergoes repeated nuclear divisions and actin relocalizations without intervening septation. At the restrictive temperature, about 35% of the *cdc10rho2* double mutant cells showed

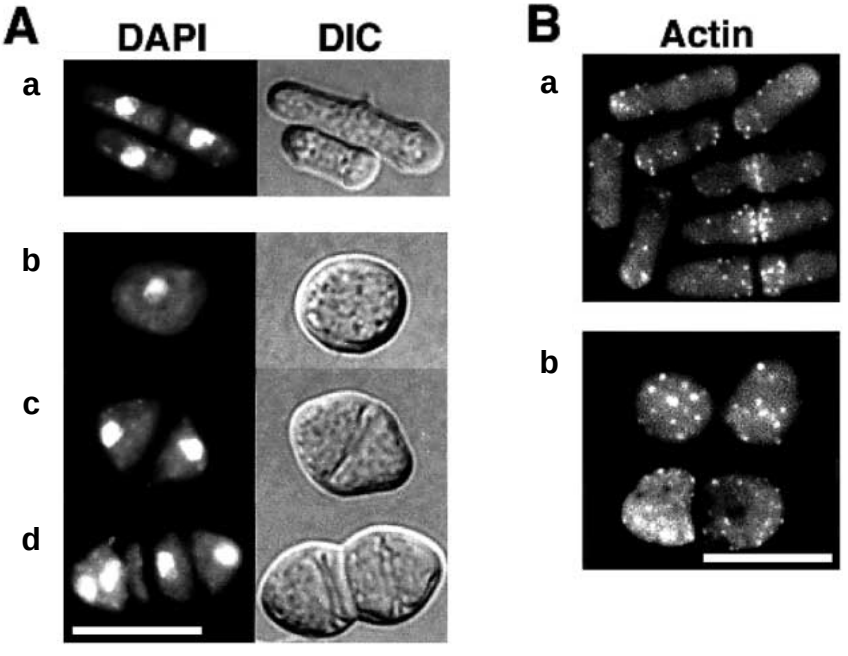

Fig. 2. Morphology and F-actin staining of the *rho2*$^+$-overexpressing cells. (A) Cell morphology. Wild-type (HM123) cells bearing pREP1-Rho2 were grown in EMM containing 4 μM thiamine at 25°C, transferred into EMM containing 4 μM thiamine (a) or EMM (b-d), cultured at 32°C for 16 hours, and fixed. The chromatin region and morphology of the cells were observed by DAPI staining (left) and DIC, differential-interference-contrast (right), respectively. (B) Localization of cortical F-actin. Wild-type cells bearing pREP1 (a) or pREP1-Rho2 (b) were grown in EMM containing 4 μM thiamine at 25°C, transferred into EMM, cultured at 32°C for 14.5 hours, fixed, and stained with rhodamine-phalloidin. Bars, 10 μm.

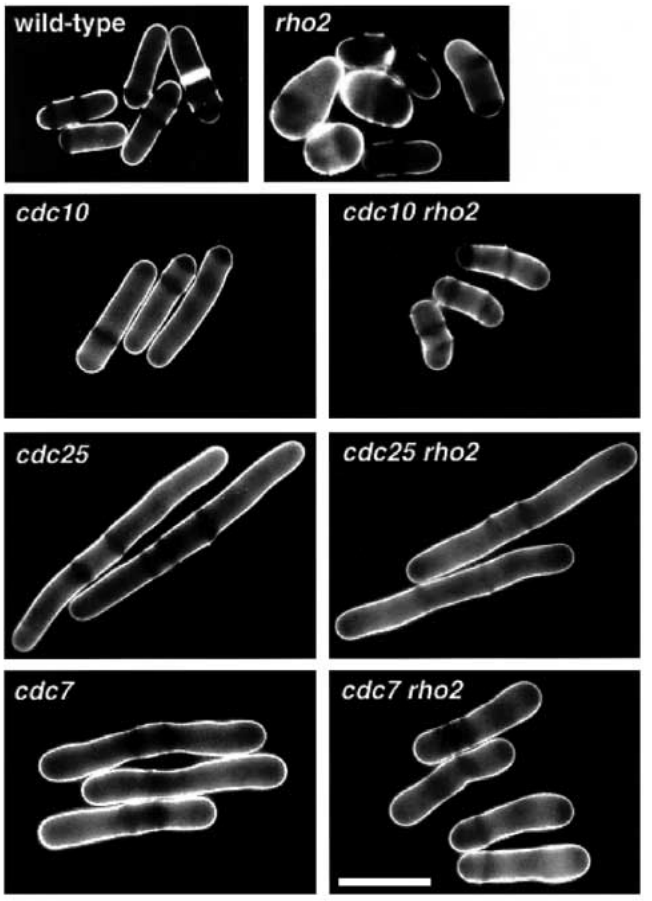

Fig. 3. Morphology of *rho2* and *cdcrho2* mutant cells. Wild-type (HM123), *rho2* disruptant (KN-1), *cdc10* (DH70-2), *cdc25* (DH71-1), *cdc7* (DH69-1), *cdc10rho2* (DH68-4), *cdc25rho2* (DH67-1), and *cdc7rho2* (DH66-1) cells were grown in YPD at 25°C, shifted to 36°C, cultured for 4.5 hours, fixed, and stained with calcofluor. Bar, 10 μm.

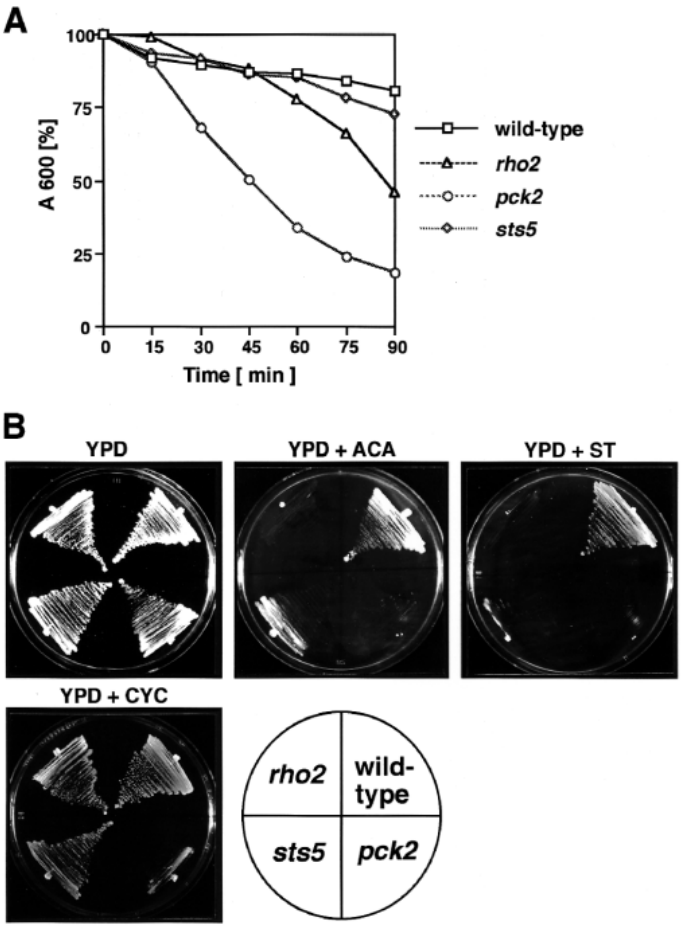

Fig. 4. Sensitivity of the *rho2* disruptant cells to glucanase treatment and to antibiotics. (A) Sensitivity to glucanase. Cells were grown in YPD at 25°C, collected, washed in water, and incubated with β-glucanase at 28°C. Time course of the changes in the turbidity at 600 nm was monitored. Turbidity at 0 time is expressed as 100% for each sample. Strains used were as follows: wild-type (open squares, HM123), *rho2* (open triangles, KN-1), *pck2* (open circles, TP47-2B), and *sts5* (open diamonds, TP40-5B). (B) Sensitivity to antibiotics. The cells were streaked on YPD plates containing 5 μg/ml aculeacin A (ACA), 2 μg/ml staurosporine (ST), or 1 μg/ml cycloheximide (CYC), and cultured at 28°C for 4 days. Strains used were as for A.

abnormal cell morphology, predominantly bent (Fig. 3). In contrast, the *cdc25rho2* double mutant cells showed a typical elongated *cdc* phenotype (Fig. 3). These results indicated that Rho2 is required for the maintenance of growth direction during monopolar growth in G_1. At the restrictive temperature, about 20% of the *cdc7rho2* double mutant cells showed abnormal cell morphology including the bent morphology (Fig. 3). The bent cells might be produced by repeated cell cycle progression in the *rho2* disruptant with a defect in cell wall integrity.

The number of nuclei in the *cdcrho2* mutant was the same as in the corresponding single *cdc* mutant: a single nucleus in *cdc10rho2* and in *cdc25rho2*, and multiple nuclei in *cdc7rho2* (data not shown).

The cell lengths of septated cells of wild-type and *rho2* disruptant were almost the same (Table 5), suggesting that the cell size control mechanism which regulates the timing between septation and cell growth is normal in *rho2* disruptant cells. However, the cell length of each *cdcrho2* double mutant was shorter than the corresponding *cdc* single mutant although the cell diameter was almost the same (Table 5). This suggests that Rho2 plays an important role in cell elongation.

Table 5. Length and diameter of *cdcrho2* double mutant cells

Strain	Cell length (μm)	Cell diameter (μm)
Wild-type*	13.5	3.5
*rho2**	13.4	3.5
cdc10	14.3	3.2
cdc10rho2	12.6	3.3
cdc25	29.7	3.7
cdc25rho2	27.4	3.5
cdc7	22.7	4.1
cdc7rho2	19.4	4.0

*Septated cells were measured.

Wild-type (HM123), *rho2* (KN-1), *cdc10* (DH70-2), *cdc10rho2* (DH68-4), *cdc25* (DH71-1), *cdc25rho2* (DH67-1), *cdc7* (DH69-1), and *cdc7rho2* (DH66-1) cells were grown in YPD at 25°C, shifted to 36°C, and cultured for 4.5 hours. The values are averages for 50 individual cells.

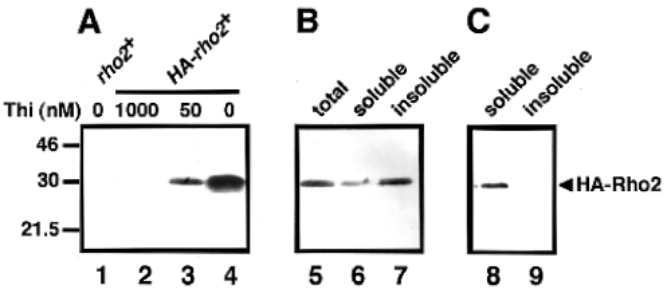

Fig. 5. Identification of the HA-Rho2 protein. (A) Exponentially growing wild-type (HM123) cells bearing either pREP1-Rho2 (*rho2*$^+$) or pREP1-HA-Rho2 (*HA-rho2*$^+$) in EMM containing 4 μM thiamine at 25°C were transferred into EMM (lanes 1 and 4) or EMM containing 1,000 nM (lane 2) or 50 nM thiamine (lane 3). After cultivation for 14 hours at 32°C, the cells were collected, disrupted with glass beads, and total cell extracts were prepared. 50 μg of the total protein samples were subjected to SDS-PAGE, and the separated proteins were processed for western blot analysis with 12CA5 as described in Materials and Methods. (B) 50 μg of the total protein sample (lane 5) prepared from the cells bearing pREP1-HA-Rho2 grown in EMM containing 50 nM thiamine were fractionated into soluble (lane 6) and insoluble fractions (lane 7) by centrifugation at 14,000 ***g***. (C) The 14,000 ***g*** insoluble fraction was resuspended in the TEG buffer containing 1% Triton X-100 for 5 minutes at room temperature. The sample was fractionated into soluble (lane 8) and insoluble (lane 9) fractions by centrifugation at 10,000 ***g***. The protein samples were subjected to SDS-PAGE and the separated proteins were processed for western blot analysis. The numbers on the left indicate M_r values of the protein markers: ovalbumin (M_r = 46,000), carbonic anhydrase (M_r = 30,000), and trypsin inhibitor (M_r = 21,500). An arrowhead indicates the position of HA-Rho2.

Identification of Rho2

To identify Rho2, the HA epitope from influenza coat protein (Wilson et al., 1984) was added to the N terminus of the coding region of the *rho2*$^+$ gene, which was driven under the thiamine-repressible *nmt1* promoter. The plasmid containing HA-tagged *rho2*$^+$ (designated pREP1-HA-Rho2) was toxic in wild-type cells grown in EMM and was capable of suppressing the drug sensitivity and the morphological defect of the *rho2* disruptant in EMM containing thiamine (data not shown). The similarity of the effects of pREP1-HA-Rho2 to those of pREP1-Rho2 indicated that HA-Rho2 functions in the cell as wild-type Rho2. Western blot analysis was performed on a total cell extract obtained from wild-type cells bearing pREP1-HA-Rho2 or pREP1-Rho2 grown in EMM. A protein of 26 kDa, the predicted molecular mass of HA-Rho2 (227 amino acid residues), was detected from the cells expressing *HA-rho2*$^+$ (Fig. 5A, lane 4) but not from the cells expressing *rho2*$^+$ (Fig. 5A, lane 1), indicating that the 26 kDa protein is HA-Rho2. The 26 kDa protein band began to accumulate 12 hours after removal of thiamine. Its level peaked at 16 hours and stayed at the high level after 22 hours (data not shown). The kinetics of this increase was in parallel with the morphological alterations seen upon induction.

To investigate the localization of Rho2 in the cell, western blot analysis was performed on soluble and insoluble fractions from wild-type cells bearing pREP1-HA-Rho2 grown under partially repressed conditions, that is, in a low concentration of thiamine, where cell growth was not affected and normal cell morphology was maintained. About 80% of HA-Rho2 was found in the insoluble fraction (Fig. 5B, lane 7), while 20% of HA-Rho2 was found in the soluble fraction (Fig. 5B, lane 6). Further, HA-Rho2 of the insoluble fraction was solubilized by treatment with 1% Triton X-100 (Fig. 5C), suggesting that HA-Rho2 is present as a membrane-bound form.

Overexpression of *rho2*$^+$ in various *cdc* mutants

The result of F-actin staining suggested that the growth polarity of the *rho2*$^+$-overexpressing cells is lost during interphase. To evaluate this possibility, we examined the effect of the overexpression of *HA-rho2*$^+$ in *cdc* mutants: *cdc10-129*, *cdc25-22*, and *cdc7-24*. The *cdc* mutant cells bearing pREP1-HA-Rho2 cultured for 10 hours after the removal of thiamine were shifted to 36°C for 4 hours. The *cdc10-129* mutant cells arrested in G_1 show a monopolar growth (Fig. 3). When *HA-rho2*$^+$ was overexpressed in the G_1-arrested mutant cells, the cells became spherical (Fig. 6A), in which cortical F-actin patches were dispersed (data not shown). When the cells cultured for 8 hours after the removal of thiamine were shifted to 36°C, the cells showed mixed phenotypes, spherical or *cdc* (data not shown). In contrast, overexpression of *rho2*$^+$ in *cdc25-22* mutant cells arrested in G_2 did not affect cell morphology (Fig. 6A). The expression levels of HA-Rho2 in these mutants were similar to each other (Fig. 6B). These

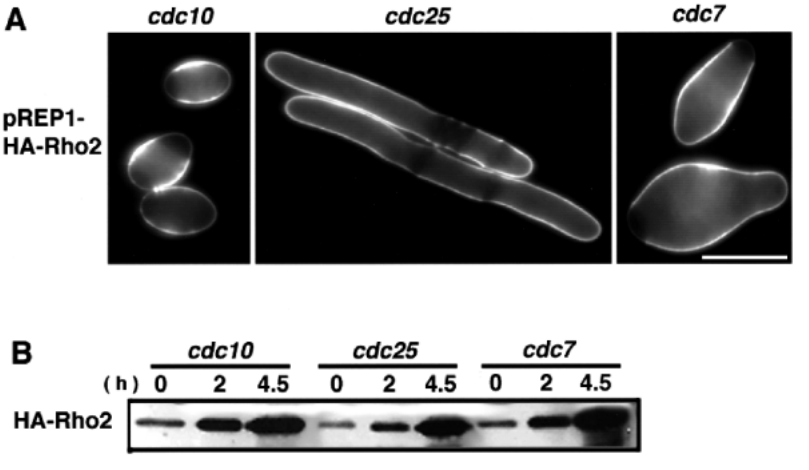

Fig. 6. Overexpression of *HA-rho2*$^+$ in various *cdc* mutants. The *cdc10* (DH70-2), *cdc25* (DH71-1), and *cdc7* (DH69-1) mutant cells bearing pREP1-HA-Rho2 were grown in EMM containing 4 μM thiamine at 25°C, transferred into EMM, cultured for 10 hours at 25°C, and shifted to 36°C. (A) Cell morphology. After cultivation for 4.5 hours at 36°C, the cells were fixed, and stained with calcofluor. Bar, 10 μm. (B) Expression level of HA-Rho2. At the indicated time (0, 2, and 4.5 hours) after shift to 36°C, the cells were collected, disrupted with glass beads, and total cell extracts were prepared. 50 μg of each of the total protein samples was processed for western blot analysis with 12CA5.

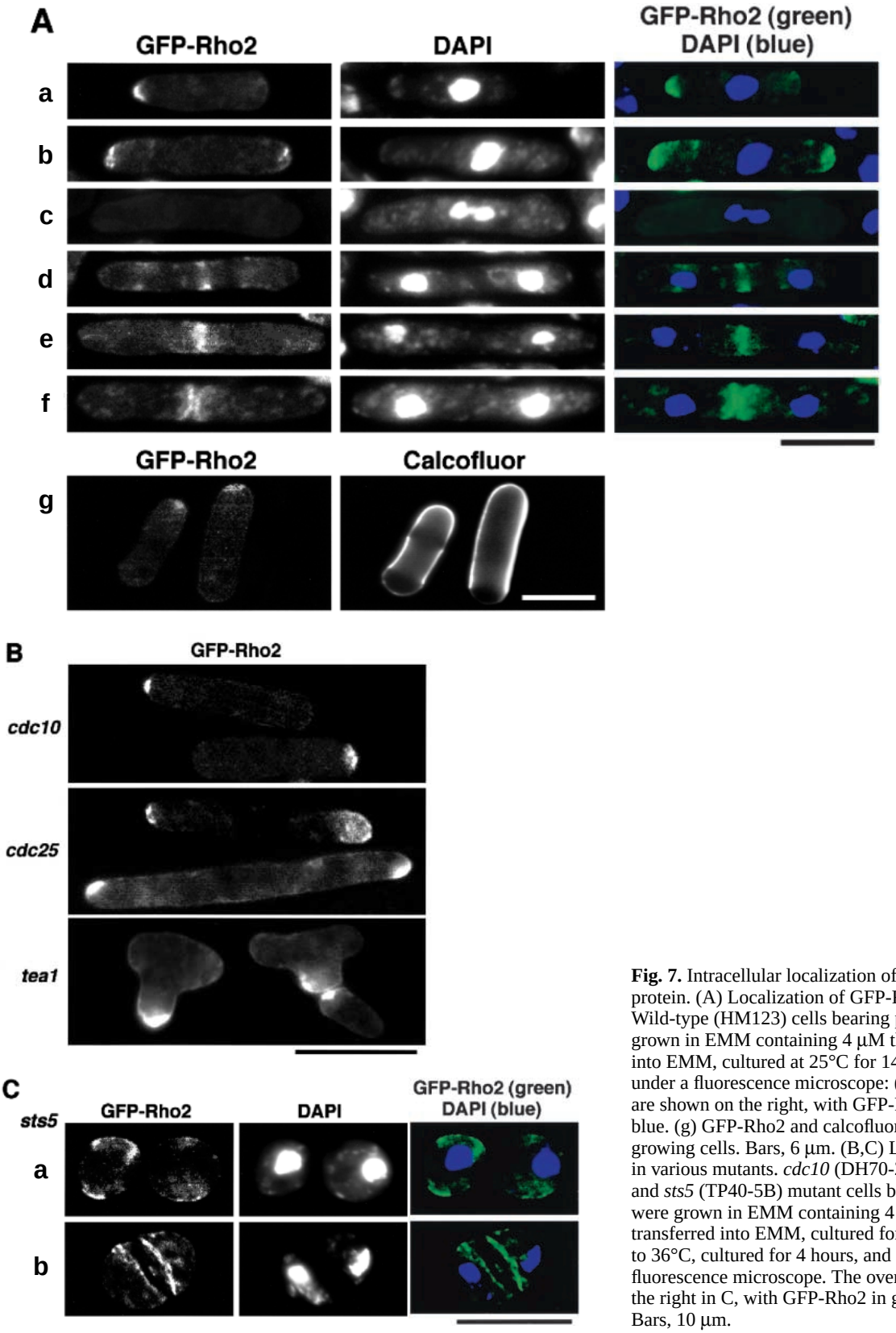

Fig. 7. Intracellular localization of the GFP-Rho2 fusion protein. (A) Localization of GFP-Rho2 in wild-type cells. Wild-type (HM123) cells bearing pREP81-GFP-Rho2 were grown in EMM containing 4 μM thiamine at 25°C, transferred into EMM, cultured at 25°C for 14.5 hours, and observed under a fluorescence microscope: (a-f) the overlaid stainings are shown on the right, with GFP-Rho2 in green and DAPI in blue. (g) GFP-Rho2 and calcofluor staining of unidirectionally growing cells. Bars, 6 μm. (B,C) Localization of GFP-Rho2 in various mutants. *cdc10* (DH70-2), *cdc25* (DH71-1), *tea1*, and *sts5* (TP40-5B) mutant cells bearing pREP81-GFP-Rho2 were grown in EMM containing 4 μM thiamine at 25°C, transferred into EMM, cultured for 11 hours at 25°C, shifted to 36°C, cultured for 4 hours, and observed under a fluorescence microscope. The overlaid stainings are shown on the right in C, with GFP-Rho2 in green and DAPI in blue. Bars, 10 μm.

results indicate that the overexpression of *rho2*$^+$ prevents the establishment of growth polarity in G_1 but does not affect the maintenance of growth polarity in G_2. When *HA-rho2*$^+$ was overexpressed in *cdc7-24* mutant cells at the restrictive temperature, the nuclear divisions repeatedly occurred (data not shown) and the cells became swollen (Fig. 6A). This result

indicates that the overexpression of *rho2*$^+$ does not affect nuclear division. The swollen cells might be produced by repeated cell cycle progression in which the establishment of growth polarity in each G_1 interfered with the overexpression of *rho2*$^+$.

Intracellular localization of Rho2

Green fluorescent protein gene (Prasher et al., 1992) was fused to the N terminus of the coding region of the *rho2*$^+$ gene, which was driven under the thiamine-repressible *nmt81* promoter. The plasmid containing GFP-fused *rho2*$^+$ (designated pREP81-GFP-Rho2) had no harmful effect in wild-type cells grown in EMM as pREP81-Rho2 (Table 4), and was capable of suppressing the phenotype of the *rho2* disruptant (data not shown). Therefore, the fusion with GFP did not interfere with the function of Rho2.

Intracellular localization of GFP-Rho2 in wild-type cells during cell cycle progression was examined (Fig. 7A). In the cells undergoing monopolar growth, GFP-Rho2 was predominantly localized at the growing end which is brightly stained by calcofluor (Fig. 7A, a and g). In the cells undergoing bipolar growth, GFP-Rho2 was localized at both ends (Fig. 7A, b). In the cells at the onset of mitosis, localization of GFP-Rho2 was unclear (Fig. 7A, c). During mitosis, GFP-Rho2 was concentrated at a medial region (Fig. 7A, d and e). After cytokinesis GFP-Rho2 was localized at the new ends of the cells produced by cytokinesis (Fig. 7A, f). We further examined the localization of GFP-Rho2 in *cdc10*, *cdc25*, and *tea1* (Snell and Nurse, 1994) mutant cells. GFP-Rho2 in *cdc10* or *cdc25* mutant cells was localized at one end, the growing end, during monopolar growth and at both ends during bipolar growth, respectively (Fig. 7B). GFP-Rho2 in *tea1* mutant cells was localized at the abnormally growing end and septation site (Fig. 7B). These results indicate that GFP-Rho2 is localized at the growing cell end(s) and the septation site.

The *sts5*$^+$ gene is essential for maintenance of growth polarity during interphase. We next examined whether the localization of GFP-Rho2 is dependent on Sts5. In *sts5* mutant cells in interphase, GFP-Rho2 was not localized in a specific region (Fig. 7C, a). However, it was localized at the septation site (data not shown) and at the new ends after cytokinesis (Fig. 7C, b), indicating that the localization of GFP-Rho2 during interphase is partially dependent on Sts5.

Functional difference between Rho2 and Rho1

To investigate a possibility of functional overlapping between Rho2 and Rho1, we examined whether Rho1 was able to suppress the phenotype of the *rho2* disruptant cells. The *rho2* disruptant cells bearing pREP1-, pREP41-, or pREP81-Rho1 were streaked on EMM or an EMM plate containing 2 μM thiamine with or without 5 μg/ml aculeacin A. The *rho2* disruptant cells could not grow in the presence of aculeacin A as described above. Under the repressed conditions, the *rho2* disruptant cells bearing pREP1-Rho2 were able to form colonies presumably because of some expression through the strong promoter, while the *rho2* disruptant cells bearing pREP1-, pREP41-, or pREP81-Rho1 could not grow. Under the derepressed conditions, the *rho2* disruptant cells bearing pREP81-Rho1 could grow slowly (Fig. 8). Therefore, the effect of suppression by *rho1*$^+$ on the drug sensitivity of the *rho2* disruptant was very weak. On the other hand, the *rho1*$^+$ gene has been shown to be essential for cell viability (Nakano et al., 1998), and *rho2*$^+$ cannot suppress the lethality of *rho1* disruptant cells. These results suggest that the functions of Rho2 and Rho1 are distinct from each other, with partial overlapping.

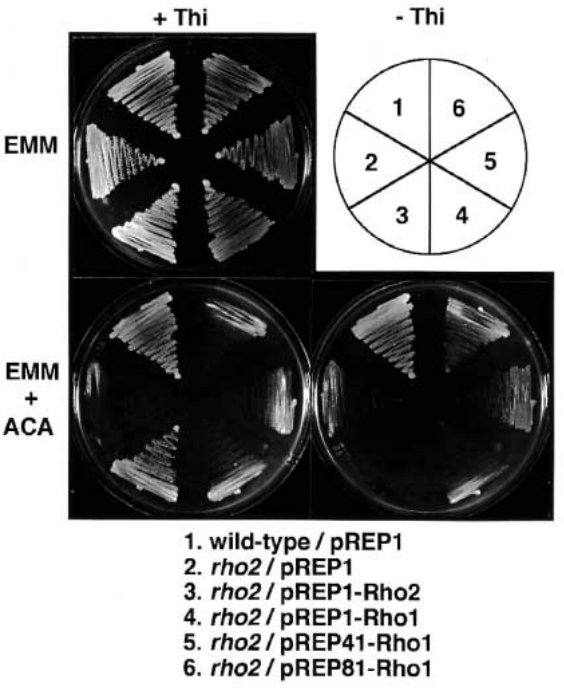

Fig. 8. Effect of the overexpression of *rho1*$^+$ on the phenotype of *rho2* disruptant cells. Cells were streaked on EMM containing 2 μM thiamine (+Thi), or EMM containing 5 μg/ml aculeacin A (ACA) with (+Thi) or without thiamine (–Thi). The plates were incubated at 28°C for 4 days. The cells used were as follows: wild-type (HM123) bearing pREP1 (1), and the *rho2* disruptant (KN-1) bearing pREP1 (2), pREP1-Rho2 (3), pREP1-Rho1 (4), pREP41-Rho1 (5), or pREP81-Rho1 (6).

DISCUSSION

To identify the genes involved in cell morphogenesis, we used a dominant genetics in which the genes causing aberrant cell morphology by overexpression were screened in a wild-type background. From this screening, a gene with a redundant function with a gene involved in cell morphogenesis or a gene causing dominant lethality by overexpression would be isolated. Indeed, *rho2*$^+$ was isolated as the gene causing lethality by overexpression. Further, our results suggested that Rho2 has a redundant function in cell morphogenesis. In the screening of recessive morphological mutants, the identification of a gene by selection of the recessive mutants will be difficult if the function of the gene is redundant with those of other genes. Thus, the identification of Rho2 by selection of the recessive mutant would be difficult. The present screening method will be complementary with an approach of analyzing recessive mutants in the identification of the genes involved in cell morphogenesis, cell cycle, and other cellular events.

What are the roles of Rho2 in cell morphogenesis and what is the target of Rho2? Our results suggested that Rho2 is involved in the control of cell wall integrity. It has been shown that one of the targets of Rho1 is 1,3-β-glucan synthase for cell wall biosynthesis in both budding and fission yeasts (Arellano et al., 1996; Drgonovå et al., 1996; Qadota et al., 1996). However, the expression of *rho1*$^+$ only weakly suppressed supersensitivity to aculeacin A of the *rho2* disruptant, suggesting that the target of Rho2 in the cell wall biosynthesis could be different from that of Rho1. Genetic analysis and the intracellular localization of GFP-Rho2 suggested that Rho2 is also involved in the control of growth polarity, including reorganization of the actin-cytoskeleton. In *S. cerevisiae*, it has been shown that Bni1, which is implicated in cytoskeletal control, is a putative target of Rho1 (Kohno et al., 1996). It would be interesting to identify a protein in *S. pombe* which has a function similar to Bni1. The *rho2* disruptant cells showed supersensitivity to staurosporine, a potent inhibitor of protein kinase C, and the cell wall integrity of the disruptant cells was also diminished. The *S. pombe pck2*$^+$ gene encoding a protein kinase C has been implicated in the control of cell wall integrity and growth polarity. The overexpression of *pck2*$^+$ in wild-type cells causes a lethal phenotype similar to that produced by overexpression of *rho2*$^+$ (Toda et al., 1993). Thus, it is possible that a functional linkage between Rho2 and protein kinase C may exist in *S. pombe* as in *S. cerevisiae* (Nonaka et al., 1995; Kamada et al., 1996). The phenotypes of various *cdcrho2* double mutants suggested that Rho2 is important for cell elongation during interphase. It is likely that Rho2 is also involved in maintenance of growth direction, which may be achieved by a complex mechanism.

GFP-Rho2 in *tea1* mutant cells was localized at abnormal growing end, suggesting that the localization of Rho2 in interphase is mediated by Tea1. In *sts5* mutant cells in interphase, GFP-Rho2 was not localized to any specific region, indicating that the localization of Rho2 in interphase is partially regulated by Sts5 which is a crucial determinant of polarized cell growth. It is important to examine how Sts5 regulates the localization of Rho2 and how Sts5 and Tea1 are functionally related. Even in *sts5* and *tea1* mutant cells, GFP-Rho2 was localized at the septation site and at the new end after cytokinesis. This result indicates that a mechanism which determines the localization of Rho2 in septum formation is different from that in interphase.

Control of the activity of Rho during cell cycle progression has not been clarified. Our results suggested that Rho2 is involved in the maintenance of growth direction in G_1 and is important for cell elongation during interphase. However, the overexpression of *rho2*$^+$ prevented the establishment of growth polarity in G_1. The control of Rho2 activity might be critical for G_1 cell cycle progression.

Our results suggested that Rho2 is involved in cell morphogenesis. However, the effect of *rho2*$^+$ disruption on cell morphogenesis is subtle. There may be other proteins which are functionally redundant with Rho2. Analyses of functional overlapping between Rho2 and Rho1 indicated that the functions of these molecules are different from each other, although the effects of the overexpression of *rho2*$^+$ and *rho1*$^+$ in wild-type cells are very similar. We presume that these G-proteins are involved in common cellular events, including control of growth polarity and cell wall integrity, but the targets of these proteins may be different.

We thank Takashi Toda, Paul Nurse, Masayuki Yamamoto, Yoshikazu Ohya, and Fulvia Verde for plasmids, strains and the cDNA library; Yukinobu Nakaseko for help with cytological techniques; and Hirofumi Nakano (Kyowa Hakko Co., Japan) for the staurosporine. We also thank Takashi Toda for constructive discussion, Paul Nurse and Mitsuhiro Yanagida for critical reading of the manuscript and useful comments, Kazuma Tanaka for discussion, and Eiko Tsuchiya, Takashi Yamada, and Ichiro Yamashita for encouragement. This work was in part supported by grants from Ministry of Education, Science, and Culture of Japan.

REFERENCES

Adams, A. E., Johnson, D. I., Longnecker, R. M., Sloat, B. F. and Pringle, J. R. (1990). *CDC42* and *CDC43*, two additional genes involved in budding and the establishment of cell polarity in the yeast *Saccharomyces cerevisiae. J. Cell Biol*. **111**, 131-142.

Alfa, C., Fantes, P., Hyams, J., McLeod, M. and Warbrick, E. (1993). *Experiments with Fission Yeast: Laboratory Course Manual*. Cold Spring Harbor Laboratory Press, Cold Spring Harbor, NY.

Arellano, M., Duran, A. and Peréz, P. (1996). Rho1 GTPase activates the (1-3)β-D-glucan synthase and is involved in *Schizosaccharomyces pombe* morphogenesis. *EMBO J.* **15**, 4584-4591.

Basi, G., Schmid, E. and Maundrell, K. (1993). TATA box mutations in the *Schizosaccharomyces pombe nmt1* promoter affect transcription efficiency but not the transcription start point or thiamine repressibility. *Gene* **123**, 131–136.

Drgonová, J., Drgon, T., Tanaka, K., Kollar, R., Chen, G. C., Ford, R. A., Chan, C. S. M., Takai, Y. and Cabib, E. (1996). Rho1p, a yeast protein at the interface between cell polarization and morphogenesis. *Science* **272**, 277-279.

Fawell, E., Bowden, S. and Armstrong, J. (1992). A homologue of the ras-related *cdc42*$^+$ gene from *Schizosaccharomyces pombe. Gene* **114**, 153-154.

Forsburg, S. L. (1993). Comparison of *Schizosaccharomyces pombe* expression systems. *Nucl. Acids Res*. **21**, 2955-2956.

Grimm, C., Kohli, J., Murray, J. and Maundrell, K. (1988). Genetic engineering of *Schizosaccharomyces pombe*: a system for gene disruption and replacement using the *ura4* gene as a selectable marker. *Mol. Gen. Genet*. **215**, 81-86.

Hall, A. (1994). Small GTP-binding proteins and the regulation of the actin cytoskeleton. *Annu. Rev. Cell Biol*. **10**, 31-54.

Ito, W., Ishiguro, H. and Kurosawa, Y. (1991). A general method for introducing a series of mutations into cloned DNA using the polymerase chain reaction. *Gene* **102**, 67-70.

Johnson, D. I. and Pringle, J. R. (1990). Molecular characterization of *CDC42*, a *Saccharomyces cerevisiae* gene involved in the development of cell polarity. *J. Cell Biol*. **111**, 143-152.

Kamada, Y., Qadota, H., Python, C. P., Anraku, Y., Ohya, Y. and Levin, D. E. (1996). Activation of yeast protein kinase C by Rho1 GTPase. *J. Biol. Chem.* **271**, 9193-9196.

Kohno, H., Tanaka, K., Mino, A., Umikawa, M., Imamura, H., Fujiwara, T., Fujita, Y., Hotta, K., Qadota, H., Watanabe, T., Ohya, Y. and Takai, Y. (1996). Bni1p implicated in cytoskeletal control is a putative target of Rho1p small GTP binding protein in *Saccharomyces cerevisiae. EMBO J*. **15**, 6060-6068.

Laemmli, U. K. (1970). Cleavage of structural proteins during assembly of the head of bacteriophage T4. *Nature* **227**, 680-685.

Madaule, P., Axel, R. and Myers, A. M. (1987). Characterization of two members of the rho gene family from the yeast *Saccharomyces cerevisiae. Proc. Nat. Acad. Sci. USA* **84**, 779-783.

Marks, J. and Hyams, J. S. (1985). Localization of F-actin through the cell division cycle of *Schizosaccharomyces pombe*. *Eur. J. Cell Biol*. **39**, 27-32.

Marks, J., Hagan, I. and Hyams, J. S. (1986). Growth polarity and cytokinesis in fission yeast: the role of the cytoskeleton. *J. Cell Sci. Suppl. 5*, 229-241.

Matsui, Y. and Toh-e, A. (1992). Yeast *RHO3* and *RHO4* ras superfamily genes are necessary for bud growth, and their defect is suppressed by a high dose of bud formation genes *CDC42* and *BEM1*. *Mol. Cell. Biol*. **12**, 5690-5699.

Matsusaka, T., Hirata, D., Yanagida, M. and Toda, T. (1995). A novel protein kinase *ssp1*$^+$ is required for alteration of growth polarity and actin localization in fission yeast. *EMBO J*. **14**, 3325-3338.

Maundrell, K. (1990). *nmt1* of fission yeast. *J. Biol. Chem.* **265**, 10857-10864.

Miller, P. J. and Johnson, D. I. (1994). Cdc42p GTPase is involved in controlling polarized cell growth in *Schizosaccharomyces pombe*. *Mol. Cell. Biol.* **14**, 1075-1083.

Mitchison, J. M. (1970). Physiological and cytological methods for *Schizosaccharomyces pombe*. In *Methods in Cell Physiology*, vol. 4 (ed. D. M. Prescott), pp. 131-165. Academic Press, New York, NY.

Mitchison, J. M. and Nurse, P. (1985). Growth in cell length in the fission yeast *Schizosaccharomyces pombe*. *J. Cell Sci*. **75**, 357-376.

Miyata, M., Kitamura, J. and Miyata, H. (1980). Lysis of growing fission-yeast cells induced by aculeacin A, a new antifungal antibiotic. *Arch. Microbiol*. **127**, 11-16.

Moreno, S., Klar, A. and Nurse, P. (1991). Molecular genetic analysis of fission yeast *Schizosaccharomyces pombe*. *Meth. Enzymol*. **194**, 795-823.

Nakano, H., Kobayashi, E., Takahashi, I., Tamaoki, T., Kuzuu, Y. and Iba, H. (1987). Staurosporine inhibits tyrosine-specific protein kinase activity of Rous sarcoma virus transforming protein p60. *J. Antibiot.* **40**, 706-708.

Nakano, K. and Mabuchi, I. (1995). Isolation and sequencing of two cDNA clones encoding Rho proteins from the fission yeast *Schizosaccharomyces pombe*. *Gene* **155**, 119-122.

Nakano, K., Arai, R. and Mabuchi, I. (1998). The small GTP-binding protein, Rho1, is a multi-functional protein that is involved in the regulation of actin localization, cell polarity, and septum formation in the yeast, *Schizosaccharomyces pombe*. *Genes to Cells* (in press).

Nonaka, H., Tanaka, K., Hirano, H., Fujiwara, T., Kohno, H., Umikawa, M., Mino, A. and Takai, Y. (1995). A downstream target of *RHO1* small GTP-binding protein is *PKC1*, a homolog of protein kinase C, which leads to activation of the MAP kinase cascade in *Saccharomyces cerevisiae*. *EMBO J*. **14**, 5931-5938.

Nurse, P. (1994). Fission yeast morphogenesis - posing the problems. *Mol. Biol. Cell*. **5**, 613-616.

Prasher, D. C., Eckenrode, V. K., Ward, W. W., Prendergast, F. G. and Cormier, M. (1992). Primary structure of the Aequorea victoria green fluorescent protein. *Gene* **111**, 229-233.

Qadota, H., Python, C. P., Inoue, S. B., Arisawa, M., Anraku, Y., Zheng, Y., Watanabe, T., Levin, D. E. and Ohya, Y. (1996). Identification of yeast Rho1p GTPase as a regulatory subunit of 1,3-β-glucan synthase. *Science* **272**, 279-281.

Rothstein, R. J. (1983). One-step gene disruption in yeast. *Meth. Enzymol*. **101**, 202-211.

Sambrook, J., Fritsch, E. F. and Maniatis, T. (1989). *Molecular Cloning: A Laboratory Manual*, 2nd edn. Cold Spring Harbor Laboratory Press, Cold Spring Harbor, NY.

Shiozaki, K. and Russell, P. (1995). Counteractive roles of protein phosphatase 2C (PP2C) and a MAP kinase homolog in the osmoregulation of fission yeast. *EMBO J*. **14**, 492-502.

Snell, V. and Nurse, P. (1993). Investigation into the control of cell form and polarity: the use of morphological mutants in fission yeast. *Development Supplement* 289-299.

Snell, V. and Nurse, P. (1994). Genetic analysis of cell morphogenesis in fission yeast : a role for casein kinase II in the establishment of polarized growth. *EMBO J*. **13**, 2066-2074.

Takai, Y., Sasaki, T., Tanaka, K. and Nakanishi, H. (1995). Rho as a regulator of the cytoskeleton. *Trends Biochem. Sci.* **20**, 227-231.

Toda, T., Shimanuki, M. and Yanagida, M. (1991). Fission yeast genes that confer resistance to staurosporine encode an AP-1-like transcription factor and a protein kinase related to the mammalian ERK1/MAP2 and budding yeast *FUS3* and *KSS1* kinases. *Genes Dev.* **5**, 60-73.

Toda, T., Shimanuki, M. and Yanagida, M. (1993). Two novel fission yeast protein kinase C-related genes of fission yeast are essential for cell viability and implicated in cell shape control. *EMBO J*. **12**, 1987-1995.

Toda, T., Niwa, H., Nemoto, T., Dhut, S., Eddison, M., Matsusaka, T., Yanagida, M. and Hirata, D. (1996). The fission yeast *sts5*$^+$ gene is required for maintenance of growth polarity and functionally interacts with protein kinase C and an osmosensing MAP-kinase pathway. *J. Cell Sci*. **109**, 2331-2342.

Verde, F., Mata, J. and Nurse, P. (1995). Fission yeast cell morphogenesis: Identification of new genes and analysis of their role during the cell cycle. *J. Cell Biol*. **131**, 1529-1538.

Wilson, I. A., Niman, H. L., Houghten, R. A., Cherenson, A. R., Connolly, M. L. and Lerner, R. A. (1984). The structure of an antigenic determinant in a protein. *Cell* **37**, 767-778.

Yaffe, M. P., Hirata, D., Verde, F., Eddison, M., Toda, T. and Nurse, P. (1996). Microtubules mediate mitochondrial distribution in fission yeast. *Proc. Nat. Acad. Sci. USA* **93**, 11664-11668.

Yamochi, W., Tanaka, K., Nonaka, H., Maeda, A., Musha, T. and Takai, Y. (1994). Growth site localization of Rho1 small GTP-binding protein and its involvement in bud formation in *Saccharomyces cerevisiae*. *J. Cell Biol*. **125**, 1077-1093.